Retrospective Clinical Research Report

Journal of INTERNATIONAL MEDICAL RESEARCH

Journal of International Medical Research
49(5) 1–15

DOI: 10.1177/03000605211004414
journals.sagepub.com/home/imr
SAGE

Long noncoding RNA LINC01296 plays an oncogenic role in colorectal cancer by suppressing p15 expression

Jianing Xu[1,2], Zhehao Zhang[1], Dong Shen[4], Ting Zhang[4], Jinsong Zhang[3,*] and Wei De[1,*]

Abstract

Objective: To examine the role of the long noncoding RNA LINC01296 in colorectal carcinoma (CRC) and to explore the underlying mechanism.

Methods: We detected LINC01296 expression levels in a cohort of 51 paired CRC and normal tissues. We also assessed the effects of LINC01296 on cell proliferation and apoptosis in CRC cells *in vitro*, and measured its effect on tumor growth in an *in vivo* mouse model. We identified the potential downstream targets of LINC01296 and assessed its regulatory effects.

Results: Expression levels of LINC01296 were elevated in 37/51 CRC tissues compared with the corresponding normal tissues and were significantly associated with tumor stage, lymph node metastasis, and distant metastasis. Knockdown of LINC01296 using antisense oligonucleotides inhibited cell proliferation and promoted apoptosis of colon cancer cells *in vitro* and inhibited tumor growth *in vivo*. Knockdown of LINC01296 also significantly increased the gene expression of p15 in colon cancer cells. LINC01296-specific suppression of p15 was validated by the interaction between enhancer of zeste homolog 2 and LINC01296.

Conclusion: Overexpression of LINC01296 suppressed the expression of p15 leading to CRC carcinogenesis. These findings may provide the basis for novel future CRC-targeted therapies.

[1]Department of Biochemistry and Molecular Biology, Nanjing Medical University, Nanjing, Jiangsu, China
[2]Department of Emergency Medicine, Jiangyin People's Hospital, Jiangyin, Jiangsu, China
[3]Department of Emergency Medicine, the First Affiliated Hospital of Nanjing Medical University, Nanjing, Jiangsu, China
[4]Department of Oncology, Jiangyin People's Hospital, Jiangyin, Jiangsu, China

*These authors contributed equally to this work.

Corresponding author:
Wei De, Department of Biochemistry and Molecular Biology, Nanjing Medical University, 101, Longmian Road, Nanjing City, Nanjing, Jiangsu 210029, China.
Email: dewei@njmu.edu.cn

Keywords
Colorectal cancer, long noncoding RNA, LINC01296, cell proliferation, cell invasion, p15

Date received: 9 February 2021; accepted: 2 March 2021

Introduction

Colorectal cancer (CRC) is the third most common cancer and the second-leading cause of cancer-related deaths worldwide. CRC development is characterized by specific molecular alterations, including gene mutations and epigenetic modifications, with mutations in genes encoding adenomatous polyposis coli, K-Ras, and p53 representing important molecular events in the development of CRC. Despite advances in the understanding of the pathogenesis of CRC, its genetic basis and the molecular mechanisms associated with CRC tumorigenesis and progression remain unclear. A better understanding of these underlying molecular mechanisms is therefore essential to allow the identification of early diagnostic markers and for the development of individualized therapies.

Recent studies have revealed that the human genome contains approximately 20,000 protein-coding genes, which cover less than 2% of the entire genome sequence,[1] and that the vast majority of the human genome (98%) comprises non-protein-coding genes.[2] Interestingly, tens of thousands of noncoding RNAs are transcribed from these noncoding genes, including ribosomal RNAs, small nucleolar RNAs, small nuclear RNAs, transfer RNAs, microRNAs, and long noncoding RNAs (lncRNAs). Increasing evidence shows that lncRNAs participate in several important cellular processes and can regulate gene expression by interacting with RNA-binding proteins, regulating RNA decay, and affecting protein stabilization.[3–5] A growing number of recent studies using high-throughput profiling and microarray technologies have revealed that lncRNAs are differentially expressed in various cancers relative to their levels in corresponding normal tissues, and play key roles in tumorigenesis and tumor progression by regulating both oncogenic and tumor-suppressive pathways.[6–8] Among these lncRNAs, LINC01296 is highly expressed in prostate cancer[9] and bladder cancer,[10] and LINC01296 knockdown was shown to inhibit prostate cancer cell proliferation, migration, and invasion.[9]

Recent studies have also revealed that LINC01296 participates in CRC tumorigenesis, progression, and prognosis.[11,12] LINC01296 was reported to be differentially expressed between CRC tissues and normal adjacent mucosal tissues.[11,12] However, other studies suggested that elevated levels of LINC01296 were associated with longer survival in patients with CRC.[13] These inconsistencies suggest the need to explore the role of LINC01296 and its associated molecular pathways in the pathology of CRC. A recent study also suggested that LINC01296 might function as a potential therapeutic target in CRC, via an unknown mechanism.[14]

In this study, we examined the role of LINC01296 in CRC. We compared its expression in CRC tissues and normal tissues and analyzed its association with tumor stage, lymph node metastasis, and distant metastasis. We also examined the effects of silencing LINC01296 on cell

proliferation, cell migration, apoptosis, and the cell cycle in colon cancer cells *in vitro* and on tumor growth in mice *in vivo*. We further investigated the effects of LINC01296 silencing on p15 and enhancer of zeste homolog 2 (EZH2) in colon cancer cells. The results will clarify the oncogenic role of LINC01296 in CRC.

Materials and methods

Cell lines and CRC tissue samples

CRC cell lines (SW480, SW620, LoVo, HT29, DLD1, and HCT116) were purchased from the Cell Resource Center of the Shanghai Institute of Life Sciences (Chinese Academy of Sciences, Shanghai, China). Cells were cultured in Dulbecco's modified Eagle medium or F12K medium (Invitrogen, Carlsbad, CA, USA) supplemented with 10% fetal bovine serum (FBS; Gibco, Invitrogen), 100 U/mL penicillin, and 100 mg/mL streptomycin in an atmosphere of 5% CO_2 at 37°C.

CRC tissues and paired normal tissues were collected from patients who underwent complete excision of primary tumors from July 2013 to December 2014 at Jiangyin People's Hospital (Jiangyin, China). No patients received preoperative chemotherapy. All tissues were maintained in liquid nitrogen. Written informed consent was obtained from all individual participants included in the study. The study protocol was approved by the Research Ethics Board of Jiangyin People's Hospital (Reference #2018-012). All procedures involving human participants were performed in accordance with the ethical standards of the institutional and/or national research committee and with the Helsinki Declaration (1964) and amendments.

RNA extraction and quantitative reverse transcription polymerase chain reaction (qRT-PCR)

Total RNA was extracted from cells or CRC tissues using TRIzol reagent (Life Technologies, Carlsbad, CA, USA) according to manufacturer's instructions. Total RNA (1 μg) was reverse-transcribed using a cDNA reverse transcription kit (Promega, Madison, WI, USA), and the relative expression levels of LINC01296 and glyceraldehyde 3-phosphate dehydrogenase (*GAPDH*) were assessed by real-time PCR using SYBR Green master mix (Life Technologies). *GAPDH* mRNA expression was used as an internal control. Specific primer information is shown in Table 1.

Cell transfection

Specific antisense oligonucleotides (ASOs; Exiqon, Vedbaek, Denmark) targeting LINC01296 (160 pmol) or negative control (NC; 160 pmol) were transfected into colon cancer cells using Lipofectamine RNAiMAX (Invitrogen). The sequences of ASO-1#, ASO-2#, and ASO-NC were 5′-AAACTGCCACAACGTA-3′, 5′-CACTG CAAAATTACTG-3′, and 5′-UUGCTTT

Table 1. Primer list.

Gene name	Forward primer	Reverse primer
LINC01296	5′-CTGGCATCATTTTCCGCTGG-3′	5′-TGATGGGTCCATTGGCAGTC-3′
GAPDH	5′-AGCCACATCGCTCAGACAC-3′	5′-GCCCAATACGACCAAATCC-3′
IRF1	5′-ATTAATTCCAACCAAATTCCAGG-3′	5′-TTGTATCGGCCTGTGTGAATG-3′
CXCL8	5′-CACTGCGCCAACACAGAAAT-3′	5′-GCCCTCTTCAAAAACTTCTCCAC-3′
p15 (*CDKN2B*)	5′-GCGCGATCCAGGTCATGATGATG-3′	5′-ACCAGCGTGTCCAGGAAGCC-3′

AACGUAAC-3′, respectively. Specific knockdown of EZH2 expression in colon cancer cells by transfection with a small-interfering RNA (siRNA) against EZH2 mRNA (200 pmol) or an NC siRNA (200 pmol) using Lipofectamine 2000 (Invitrogen). The EZH2 siRNA sequence was 5′-GAGGUUCAGACGAGCUGAU UU-3′, and the si-NC sequence was 5′-CGUUAATACCUUGAATTUUAA-3′.

Cell proliferation and colony-formation assays

Cell proliferation was measured by 3-(4,5-dimethylthiazole-2-yl)–2,5-diphenyltetrazolium bromide (MTT) assay (Thermo Fisher Scientific, Waltham, MA, USA) according to the manufacturer's instructions. The absorbance at 490 nm was measured using a multiwall scanning spectrophotometer (Bio Rad, Hercules, CA, USA). For colony-formation assays, SW480 and LoVo cells were seeded in 6-well plates and monitored for 2 weeks. Clones were stained with a solution of 1% crystal violet for 30 minutes, washed with distilled water, and air dried, after which the numbers of colonies in each well were determined in a blinded manner with respect to the sample identity. Each cell line was assayed in triplicate.

Cell cycle and apoptosis analyses

LoVo and SW480 cells were transfected with LINC01296 ASOs or ASO-NC and then harvested. The cells were then stained with propidium iodide (PI) using a cycle TEST^{TM} PLUS DNA reagent kit (BD Biosciences, San Jose, CA, USA) according to manufacturer's protocol, and analyzed using a FACScan flow cytometer (BD Biosciences). The percentages of cells in the G0/G1, S, and G2/M phases were calculated. Apoptosis was detected using an Annexin V-fluorescein isothiocyanate (FITC) apoptosis detection kit (Qiagen, Hilden, Germany). Briefly, cells were collected after digestion with 0.25% trypsin in the absence of EDTA and rinsed. The cells were re-suspended in binding buffer with 5 μL of FITC antibody and 5 μl PI. After incubation in the dark for 10 minutes at room temperature, FITC and PI staining were measured by flow cytometry.

Transwell assay

Cell migration assays were performed in Transwell chambers (BD Biosciences) at 48 hours post-transfection. Cells (2.5×10^4) were suspended in 200 μL of serum-free medium and seeded in the upper chamber, and culture medium (500 μL) containing 10% FBS was placed into the bottom chamber. After incubation at 37°C for 24 hours in a humidified atmosphere of 5% CO_2, the cells on the upper surfaces of the chambers were removed using cotton swabs. Cells on the bottom surfaces of the chambers were fixed with polyoxymethylene and stained with 0.1% crystal violet for 20 minutes. The invading cells were counted in five randomly selected fields under a microscope, and the average value was calculated. Each experiment was conducted in triplicate.

RNA sequencing and data analysis

cDNA libraries for single-end sequencing were prepared using the Ion Total RNA-seq kit, v2.0 (Life Technologies). Samples were diluted and mixed, and the mixture was processed using a OneTouch 2 instrument (Life Technologies) and enriched on a OneTouch 2 ES station (Life Technologies) to prepare template-positive Ion PI ion sphere particles (Life Technologies) using the Ion PI Hi-Q OT2 200 kit (Life Technologies). After enrichment, the mixed template-positive Ion PI ion sphere particles for each sample were loaded onto

a P1v3 Proton Chip (Life Technologies) and sequenced on an Ion Proton sequencer using the Ion PI Hi-Q sequencing 200 kit (Life Technologies). The DESeq algorithm was used to identify differentially expressed genes. Gene Ontology (GO) analysis was performed to elucidate the biological implications of the differentially expressed genes. We also validated the expression of changed genes in SW480 and LoVo cells following LINC01296 downregulation by qRT-PCR.

Fluorescence in situ hybridization (FISH) and fractionation

LoVo and SW480 cells were fixed in 4% formaldehyde for 10 minutes and washed with phosphate-buffered saline (PBS) for 5 minutes. Fixed cells were permeabilized for 10 minutes in PBS containing 0.5% Triton-X 100, followed by incubation at 37°C with pre-hybridization solution for 30 minutes. The cells were then incubated overnight at 37°C with probe-hybridization solution, and each slide was washed with hybridization washing buffer and dehydrated. The air-dried slides were stained with 4′,6-diamidino-2-phenylindole (DAPI) for detection. Ribo FISH kit and Ribo lncRNA FISH probe mix were purchased from Ribo (Guangzhou, China). The sequences of the probes used in this study are presented in Table 1. Cytoplasmic and nuclear RNA were isolated using a PARIS kit (Life Technologies) according to the manufacturer's protocol.

RNA immunoprecipitation (RIP) assay

RIP was used to determine if LINC01296 could interact or bind with EZH2 in SW480 cells (SW480 cell line). RIP assays were performed using an EZMagna RIP kit (Cat: 17-704; Millipore, Billerica, MA, USA) according to the manufacturer's protocol. RIP lysis buffer was included in the EZMagna RIP kit. SW480 cells were lysed in lysis buffer, and the extract was incubated for 6 hours at 4°C together with magnetic beads conjugated to antibodies recognizing EZH2 or control IgG (Millipore). The beads were then washed and incubated with proteinase K to remove proteins. Purified RNA was subjected to qRT-PCR to determine the presence of LINC01296 using specific primers.

Western blot analysis

Colon cancer cells (SW480 cell line) were harvested and washed with cold PBS and the cell pellets were lysed in 0.1 mL buffer (20 mM Tris-HCl (pH 7.5), 150 mM NaCl, 1% Triton X-100, 1% sodium pyrophosphate, and protease inhibitor cocktail). The supernatant was collected after centrifugation at $14{,}000 \times g$ for 20 minutes at 4°C. Protein concentrations were determined using a BCA protein assay kit (Thermo Fisher Scientific). Aliquots of the cleared supernatant containing total protein (25 μg) were resolved on a 15% acrylamide gel and subsequently transferred to a polyvinylidene fluoride membrane. The protein bands were visualized using an enhanced chemiluminescence detection kit (Millipore).

Chromatin immunoprecipitation (ChIP) assay

CRC cells were treated with formaldehyde and incubated for 10 minutes to generate DNA-protein cross-links. ChIP experiments were carried out using an EZ-Magna ChIPA kit (catalog number 17-408; Millipore). Cell lysates were sonicated to generate chromatin fragments of 200 to 300 bp in length and immunoprecipitated with anti-EZH2, anti-trimethyl-histone H3 (Lys27), and IgG antibodies (Millipore). Precipitated chromatin DNA was recovered and analyzed by qRT-PCR. The primer sequences targeted the p15 promoter region.

Animals used for in vivo *experiments*

Four-week-old male nude mice were purchased from the Animal Center of Nanjing University (Nanjing, China). All the animal were kept under standard animal-room conditions (26–28°C, 40%–60% humidity, and a uniform dark-light cycle), under pathogen-free conditions. All the animal experiments were conducted at Nanjing Medical University. All animal care and experimental protocols complied with the Animal Management Rules of the Ministry of Health of the People's Republic of China and were approved by the Institutional Animal Care and Use Committee of Nanjing Medical University (Approval No. IACUC-1601289).

Tumor-formation assay

Eight nude mice were divided randomly into two groups. SW480 cells were transfected with ASO-#1 or ASO-NC, harvested, washed with PBS, and re-suspended at 2×10^7 cells/mL. Suspended cells (100 μL) were injected into the lower right flank of each mouse. We then observed tumor formation in the nude mice and recorded the tumor size every 3 days. The mice were finally sacrificed by cervical dislocation at 18 days post-injection. The tumors were removed, photographed, and weighed, and then fixed in formaldehyde for pathological examination. Xenograft tumor tissues were subjected to hematoxylin and eosin staining and immunohistochemical staining to assess Ki-67 expression (Serbicebio Technology Co., Wuhan, China).

Statistical analysis

All experiments were performed in triplicate, and results are presented as the mean ± standard deviation. Data were analyzed by Student's *t*-test and one-way or two-way analysis of variance. $P < 0.05$ was considered significant. All statistical analyses were performed using SPSS for Windows, Version 16.0 (SPSS Inc., Chicago, IL, USA). No post-hoc analysis was performed because of the limited number of experiments.

Results

LINC01296 expression in CRC tissues and its clinical significance

We obtained CRC and paired normal tissue samples from 51 patients. The characteristics of the patients are presented in Table 2. We measured LINC01296 expression levels in the paired CRC and normal tissues by qRT-PCR. LINC01296 was highly expressed in 37 of 51 CRC tissue samples ($P = 0.001$) (Figure 1a). Moreover, LINC01296 expression was positively associated with tumor TNM stage ($P = 0.001$), lymph node metastasis ($P = 0.025$), and distant metastasis ($P = 0.039$) (Figure 1b–d), and negatively associated with survival

Table 2. Correlation between LINCO1296 expression and clinicopathologic parameters in patients with colorectal cancer.

	LINCO1296		
Parameter	Low expression	High expression	*P*-value
Age (years)			
≤50	2	8	0.707
>50	12	29	
Sex			
Male	7	19	>0.95
Female	7	18	
T stage			
T1+T2	13	15	0.001
T3+T4	1	22	
Lymph node metastasis			
Negative	12	18	0.025
Positive	2	19	
Distant metastasis			
M0	13	22	0.039
M1	1	15	

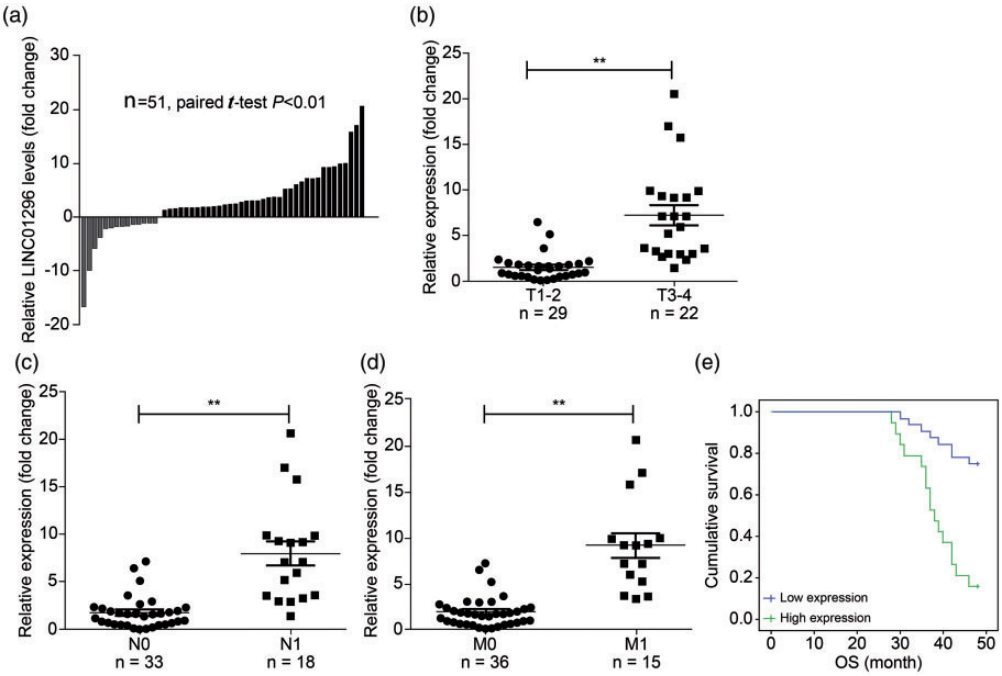

Figure 1. LINC01296 expression in colorectal cancer (CRC) tissues and its clinicopathological significance. (a) Heat map showing differentially expressed long noncoding RNAs (lncRNAs) found in CRC tissues according to The Cancer Genome Atlas data (https://portal.gdc.cancer.gov/). (b) Relative LINC01296 expression levels in paired CRC and normal tissues from 51 patients determined by quantitative reverse transcription-polymerase chain reaction. (c–e) Elevated LINC01296 expression was positively associated with tumor stage, lymph node metastasis, and distant metastasis in CRC. High LINC01296 expression was negatively associated with survival rate. $^{**}P < 0.01$. Triplicate experiments were conducted.
OS, overall survival.

($P < 0.001$) (Figure 1e). These findings indicated that LINC01296 might play an important role in CRC development and progression.

LINC01296 knockdown inhibited colon cancer cell proliferation and cell cycle progression

We explored the potential biological function of LINC01296 in CRC by examining its expression levels in six colon cancer cell lines (LoVo, SW480, SW620, HT29, HCT116, and DLD1). LINC01296 expression was high in LoVo, SW480, SW620, and HT29 cells, but low in HCT116 and DLD1 cells (Figure 2a). Considering both the availability and feasibility of these cell lines, we selected SW480 and LoVo cells with relatively high LINC01296 expression levels for subsequent experiments.

To study the role of LINC01296 in more detail, we transfected SW480 and LoVo cells with specific ASOs targeting LINC01296 mRNA. qRT-PCR revealed significant inhibition of LINC01296 in both SW480 and LoVo cells ($P < 0.001$) (Figure 2b). We then evaluated the effects of LINC01296 knockdown on cell proliferation by MTT assay. Down-regulation of LINC01296 significantly decreased cell growth compared with control cells

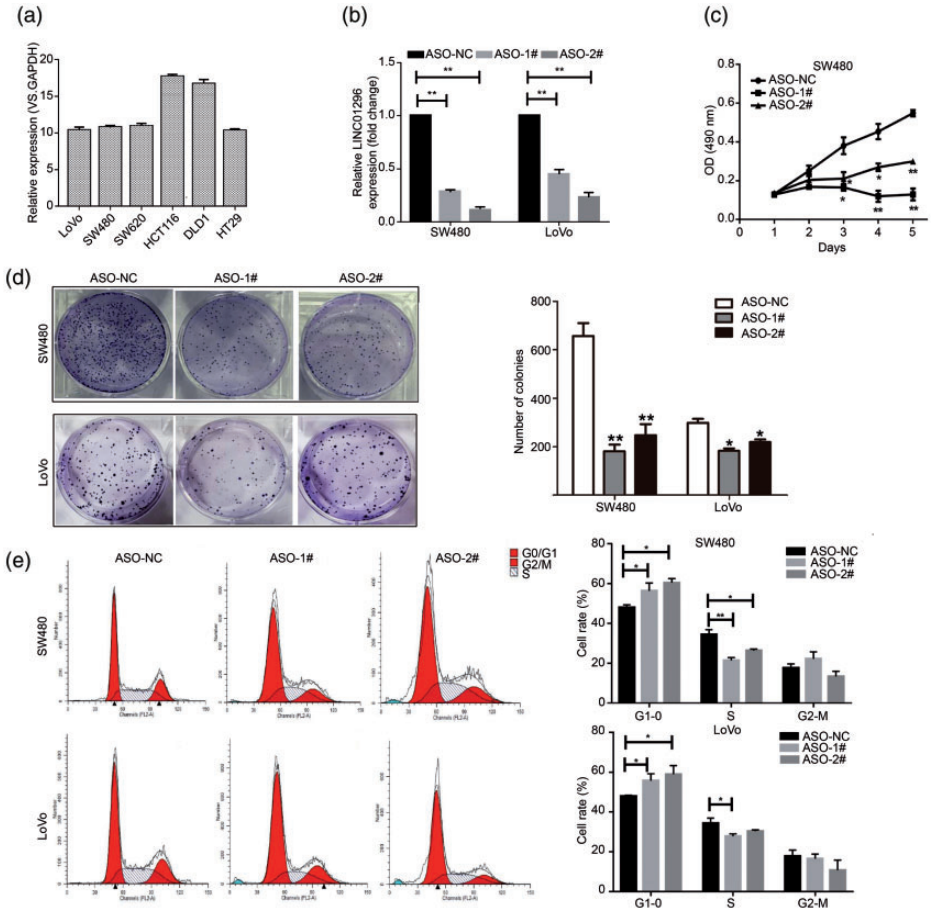

Figure 2. LINC01296 knockdown inhibited colon cancer cell proliferation and colony formation. (a) LINC01296 relative expression levels in LoVo, SW480, SW620, HT29, HCT116, and DLD1 cells detected by quantitative reverse transcription-polymerase chain reaction (qRT-PCR). (b) Relative LINC01296 expression levels in LoVo and SW480 cells after transfection with LINC01296 or negative control (NC) antisense oligonucleotides (ASOs) detected by qRT-PCR. (c) Growth curves for LoVo and SW480 cells transfected with LINC01296 or NC ASOs determined by MTT assays. Cell viability was tested by MTT assay after transfection with LINC01296 or NC ASOs for 48 hours. (d) Colony formation was decreased in LoVo and SW480 cells transfected with LINC0196 ASOs compared with cells transfected with NC ASO. (e) Flow cytometric detection of the percentage of cells in G0/G1, S, and G2/M phases in LoVo and SW480 cells after transfection with LINC01296 or NC ASOs. $^{**}P<0.01$; $^{*}P<0.05$. Triplicate experiments were conducted.

($P < 0.05$, $P < 0.01$) (Figure 2c). Similarly, transfection with LINC0196 ASOs significantly reduced the numbers of SW480 and LoVo cell clones in colony-formation assays compared with control cells ($P < 0.05$ LoVo, $P < 0.01$ SW480) (Figure 2d).

We also examined the effects of LINC01296 on the cell cycle distribution by flow cytometry. LINC01296 downregulation induced significant G0/G1 phase arrest ($P < 0.05$) and decreased the percentage of cells in S phase ($P < 0.05$, $P < 0.01$),

but had no significant effect on the percentages of cells in G2/M phase (Figure 2e).

LINC01296 knockdown induced cell apoptosis and inhibited colon cancer cell migration

We determined the effect of LINC01296 on apoptosis in CRC cells by flow cytometry assays of SW480 and LoVo cells transfected with LINC01296 ASOs or ASO NC. Apoptosis was significantly increased in SW480 and LoVo cells transfected with LINC01296 ASO-1# and ASO-2# compared with control cells ($P < 0.05$ and $P < 0.01$) (Figure 3a, b). In addition, LINC01296 knockdown inhibited the migration of SW480 and LoVo cells 24 hours after transfection compared with cells transfected with ASO-NC control, as shown by Transwell chamber assay ($P < 0.05$, $P < 0.01$) (Figure 3c, d).

LINC01296 knockdown inhibited colon cancer growth in vivo

To confirm if LINC01296 affected tumor growth, we inoculated nude mice with SW480 cells transfected with LINC01296 ASO-#1 or ASO NC and sacrificed them at 18 days post-injection. The growth curves showed that LINC01296 downregulation significantly inhibited tumor growth *in vivo* ($P < 0.01$) (Figure 4a, b). Tumor weight and LINC01296 expression level were both significantly lower in the LINC01296 ASO-#1 group compared with the NC group ($P < 0.01$ and $P < 0.05$,

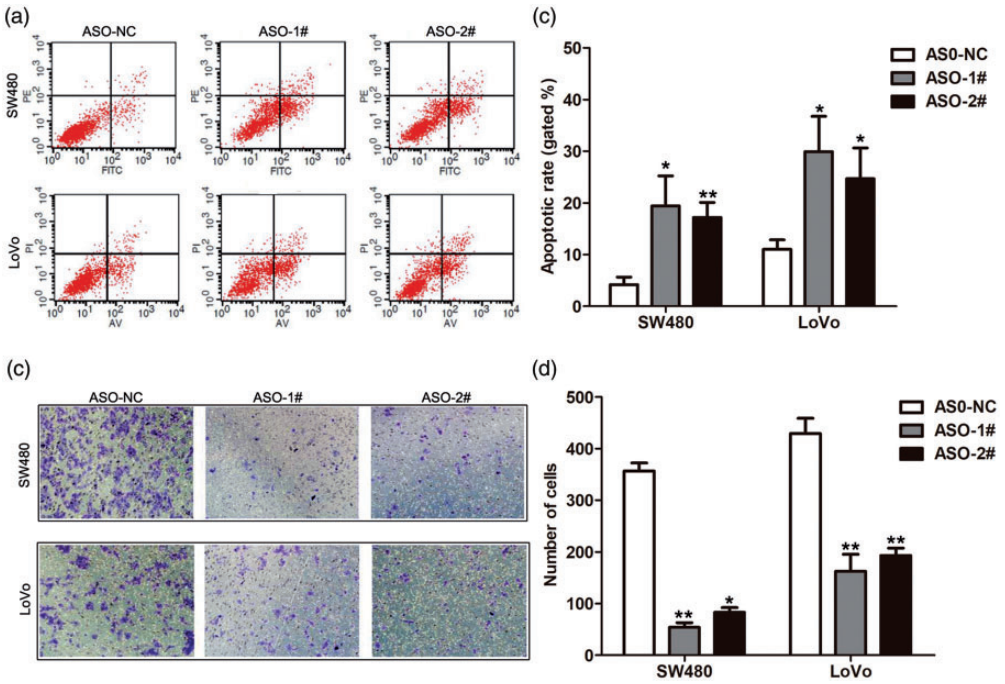

Figure 3. Effect of LINC01296 on colon cancer cell apoptosis and migration. LoVo and SW480 cells were transfected with LINC01296 or negative control (NC) antisense oligonucleotides (ASOs). (a, b) Flow cytometric detection of percentages of apoptotic LoVo and SW480 cells following ASO transfection. (c, d) Transwell assays were performed to examine the migratory abilities of LoVo and SW480 cells after transfection with LINC01296 or NC ASOs. Triplicate experiments were conducted. $^{**}P < 0.01$; $^{*}P < 0.05$.

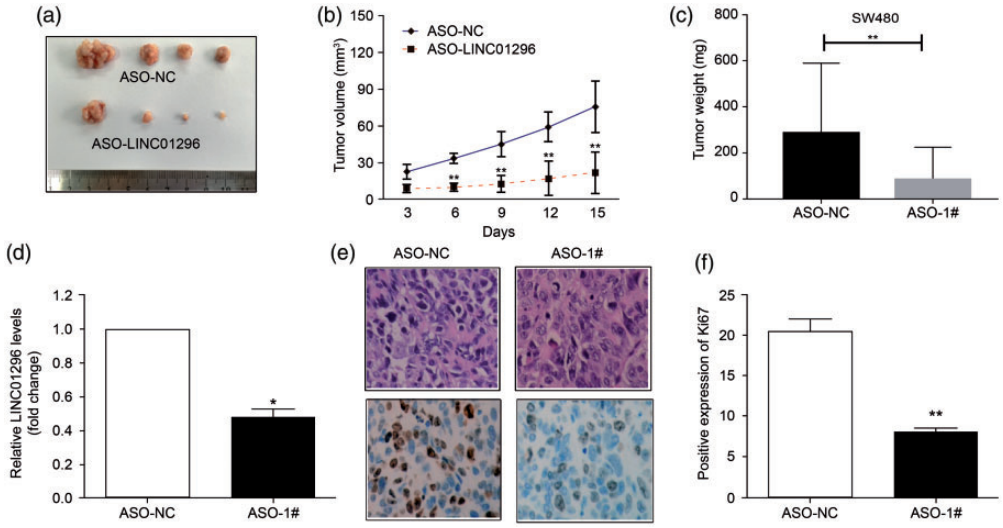

Figure 4. LINC01296 knockdown inhibited colorectal cancer tumorigenesis *in vivo*. (a) Tumor diameters in the LINC01296 antisense oligonucleotide (ASO) group were significantly smaller than those in the negative control (NC) group. (b) Tumor growth curves for the LINC01296 and NC ASO groups. (c) Tumor weights were significantly lower in the LINC01296 ASO group compared with the NC ASO group. (d) Relative LINC01296 expression levels in tumor tissues from LINC01296 and NC ASO mice determined by quantitative reverse transcription-polymerase chain reaction. (e, f) Immunohistochemical assays showed that expression of the proliferation-index factor Ki67 was lower in the LINC01296 ASO-#1 group than in the control group. $^{**}P < 0.01$; $^{*}P < 0.05$. Triplicate experiments were conducted.

respectively) (Figure 4c, d). Furthermore, expression of the proliferation-index factor Ki-67 was also significantly lower in the LINC01296 ASO-#1 group than in the control group ($P < 0.01$) (Figure 4e, f).

Differentially expressed genes following LINC01296 downregulation

We performed next-generation sequencing of SW480 cells transfected with LINC01296 ASO or ASO NC to identify potential downstream targets of LINC01296 in CRC cells. Expression levels of 1950 genes were altered in SW480 cells transfected with LINC01296 ASO-#1 compared with control cells (Figure 5a). Additionally, Gene Ontology (GO) and pathway enrichment analyses revealed that these differentially expressed genes were enriched in functions including gene expression regulation, the Notch signaling pathway, and cell cycle regulation (Figure 5b). Following LINC01296 knockdown, 26 up-regulated genes were identified in SW480 cells, corresponding to gene products involved in cell cycle regulation. Among these, p15, interferon regulatory factor 1, and C-X-C motif chemokine ligand 8 play roles in both cell cycle arrest and negative regulation of cell proliferation (Figure 5c). Furthermore, we validated the elevation of p15 expression in both SW480 and LoVo cells following LINC01296 downregulation (Figure 5d), and we therefore selected p15 as a target gene for additional study.

LINC01296 repressed p15 transcription through interactions with EZH2

We investigated the mechanism by which LINC01296 regulated p15 expression in

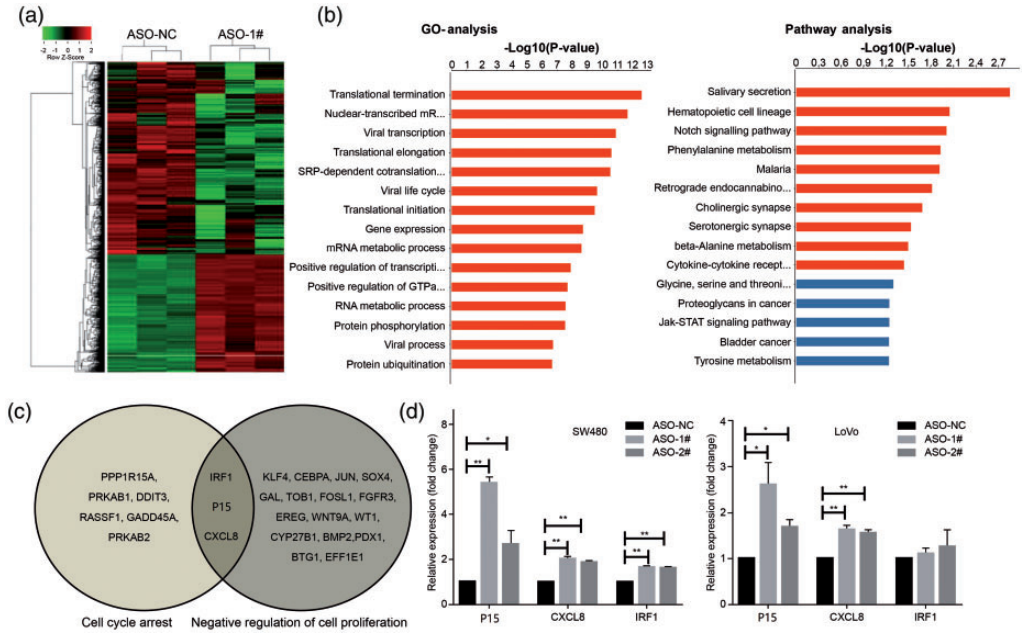

Figure 5. Identification of downstream targets of LINC01296 in colorectal cancer cells. (a) Heat map showing 1950 differentially expressed genes in SW480 cells transfected with LINC01296 antisense oligonucleotides (ASOs) relative to expression levels in the control group, identified by RNA sequencing. (b) Gene Ontology and pathway analyses of differentially expressed genes. (c) Overlap analyses of genes enriched for roles in cell cycle arrest and negative regulation of cell proliferation pathways. (d) Relative expression levels of p15, interferon regulatory factor 1, and C-X-C motif chemokine ligand in LoVo and SW480 cells transfected with LINC01296 or negative control ASOs detected by quantitative reverse transcription-polymerase chain reaction. $^{**}P < 0.01$; $^{*}P < 0.05$. Triplicate experiments were conducted NC, negative control; IRF1, interferon regulatory factor 1; CXCL8, C-X-C motif chemokine ligand 8.

CRC cells by examining the subcellular distribution of LINC01296 in SW480 and LoVo cells. LINC01296 was mainly localized in the nucleus, according to FISH and cytoplasmic and nuclear RNA-isolation analyses (Figure 6a, b). Recent studies identified lncRNAs that interacted with EZH2 to downregulate expression of the tumor suppressor gene p15.[15] In the present study, RIP showed that LINC01296 could also bind to the EZH2 protein in SW480 cells (Figure 6c). We then transfected cells with EZH2 siRNA to downregulate its expression, and qRT-PCR verified significant siRNA-mediated decreases in EZH2 levels in SW480 and LoVo cells. Interestingly, EZH2 knockdown significantly increased p15 mRNA expression levels in SW480 and LoVo cells ($P < 0.01$ and $P < 0.05$, respectively) (Figure 6d). These results were confirmed by western blotting (Figure 6e). These findings suggested that LINC01296 inhibited p15 levels by binding to the EZH2 protein.

We then designed a set of primers specific for the p15 promoter region and performed ChIP analysis using anti-EZH2 and anti-trimethyl-histone H3 (Lys27) antibodies. LINC01296 knockdown decreased EZH2 and histone H3 with trimethylated lysine 27 (H3K27me3) binding to the p15 promoter (Figure 6f), suggesting that

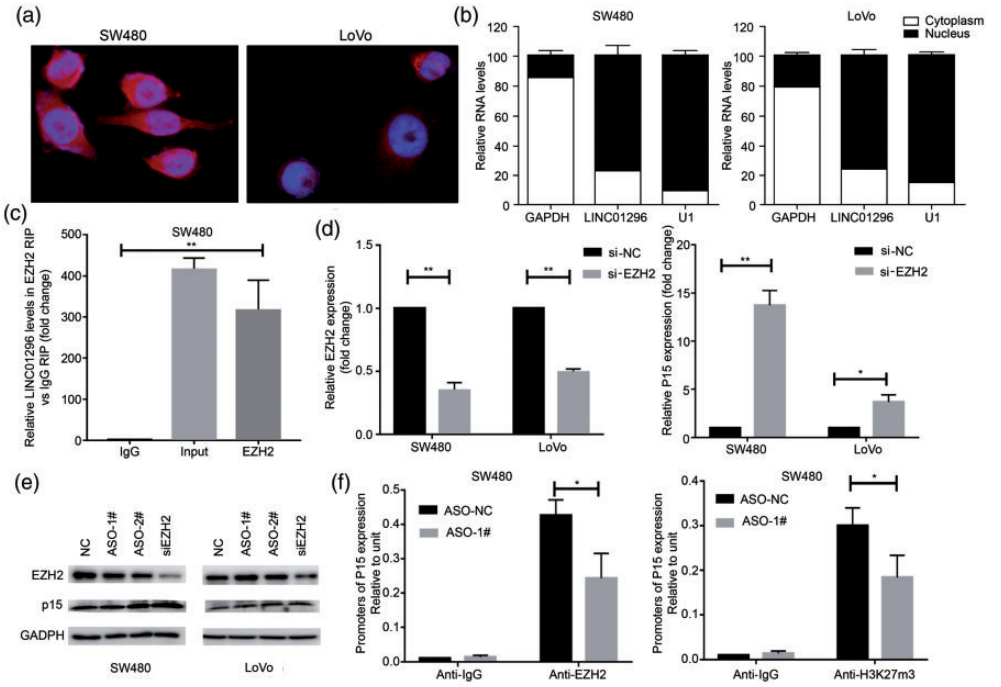

Figure 6. LINC01296 represses p15 gene expression by interacting with EZH2. (a) Fluorescence *in situ* hybridization analysis of subcellular distribution of LINC01296 in SW480 and LoVo cells. Red, LINC01296 probe signal; blue, DAPI signal. (b) Cytoplasmic:nuclear expression ratios of LINC01296 in SW480 and LoVo cells detected by quantitative reverse transcription-polymerase chain reaction (qRT-PCR). (c) RNA immunoprecipitation results showed relative enrichment of LINC01296 RNA bound to EZH2 compared with levels bound to IgG. (d) Relative EZH2 and p15 mRNA expression levels in SW480 and LoVo cells transfected with EZH2 small interfering RNA (siRNA) detected by qRT-PCR. (e) Relative EZH2 and p15 protein expression levels in SW480 and LoVo cells transfected with EZH2 siRNA or LINC01296 antisense oligonucleotides detected by western blotting. (f) Chromatin immunoprecipitation assay demonstrated that LINC01296 knockdown decreased EZH2 binding and H3K27me3 in the p15 promoter. $^{**}P<0.01$; $^{*}P<0.05$. Triplicate experiments were conducted.
ASO, antisense oligonucleotide; NC, negative control; RIP, RNA immunoprecipitation; GAPDH, glyceraldehyde 3-phosphate dehydrogenase.

LINC01296 might repress p15 levels in CRC cells, at least in part by interacting with EZH2.

Discussion

In the present study, we demonstrated that LINC01296 expression levels were increased in CRC. Down-regulation of LINC01296 inhibited cell proliferation and migration i*n vitro* and tumor growth *in vivo*, and promoted colon cancer cell apoptosis and cell cycle arrest *in vitro*. LINC01296 also functioned as an oncogene by suppressing p15 expression by interacting with EZH2 in CRC.

LINC01296 is implicated in the pathology of certain human cancers, including prostate cancer, bladder cancer, and CRC.[13] However, its expression patterns, clinicopathological significance, and functional roles in CRC have not been fully elucidated. In this study, we showed that LINC01296 expression was significantly

up-regulated in most colon cancer cell lines and in CRC tissues, with high expression levels associated with tumor stage, lymph node metastasis, and distant metastasis in patients with CRC. Our results also suggested that LINC01296 might play an oncogenic role in CRC. The expression of LINC01296 was negatively correlated with patient survival, which was inconsistent with the findings of Qiu et al.,[13] who reported that elevated LINC01296 levels were associated with better overall survival rates in patients with CRC, based on several published datasets derived from the Gene Expression Omnibus database. However, functional studies of LINC01296 in prostate and bladder cancer tissues support an oncogenic role for LINC01296 in tumorigenesis.[9,10]

In the present study, LINC01296 knockdown inhibited colon cancer cell proliferation, migration, and invasion, and promoted apoptosis and induced cell cycle arrest *in vitro*, and inhibited tumor growth *in vivo*. In addition, LINC01296 downregulation altered the expression levels of thousands of genes in CRC cells, including those enriched in cell proliferation, cell cycle progression, and transcription.

The current study also showed that expression of the cell cycle regulator p15 was significantly up-regulated in SW480 cells following LINC01296 knockdown. p15 acts as a tumor suppressor in various human cancers, including pancreatic cancer, malignant melanoma, leukemia, maxillofacial squamous cell carcinoma, prostate cancer, breast cancer, and lung cancer.[16,17] Recent studies revealed that the p15 gene was inactivated by genomic deletion, mutation, and hypermethylation of the promoter region in a variety of human cancers.[18,19] Additionally, Kudoh et al.[20] identified p15 and p16 gene deletions in ovarian cancers using PCR and analyzed the relationship between gene activation and sensitivity to chemotherapy, reporting homozygous p15 deletions in 33% of primary epithelial ovarian cancer cases. Hypermethylation is another important epigenetic mechanism involved in p15 silencing in human cancers. Ishiguro et al.[21] investigated the methylation of the p15 gene in CRC using methylation-specific PCR, and revealed aberrant p15 promoter methylation in 26% of tumor tissues compared with only 2.4% of normal mucosae.

In addition to genetic alterations and promoter DNA CpG methylation, p15 transcription could also be repressed by LINC01296 in CRC cells by a process mediated by the histone methyltransferase EZH2. EZH2 is a subunit of the polycomb repressor complex 2 and plays oncogenic roles in human cancers.[22,23] EZH2 was recently found to induce transcriptional silencing of tumor suppressor genes (including p15) via H3K27me3.[24,25] Our results revealed that p15 expression increased after downregulation of both LINC01296 and EZH2. Furthermore, RIP assays confirmed that LINC01296 could bind to EZH2, and ChIP assays confirmed that EZH2 could bind to the p15 promoter and that H3K27me3 modifications decreased following LINC01296 downregulation. These findings indicate that LINC01296 might contribute to CRC cell proliferation and cell cycle progression in a manner partially dependent upon the repression of p15 expression.

This study had several limitations that need to be addressed in future experiments. First, our experiments focused on cell lines with high LINC01296 expression (LoVo and SW480 cell lines), and further experiments using more cell lines, including low-expressing cell lines, should be carried out to confirm the results of this study. Second, the specific nuclear localization on LINC01296 should be verified by nucleus–cytoplasm WB assay

In summary, our results revealed that LINC01296 is highly expressed in CRC

cells and CRC tissues, and that high levels of LINC01296 expression are associated with tumor stage, lymph node metastasis, and distant metastasis. Additionally, LINC01296 knockdown inhibited colon cancer cell proliferation, migration, and invasion *in vitro* and slowed tumor growth *in vivo*. Furthermore, LINC01296 functions as an oncogene by suppressing p15 expression by interacting with EZH2 in CRC. Our findings indicate that expression of LINC01296 could be a marker for CRC progression, with potential implications for targeted therapy.

Declaration of conflicting interest

The authors declare that there is no conflict of interest.

Funding

The author(s) disclosed receipt of the following financial support for the research, authorship, and/or publication of this article: This study was partly supported by Wuxi Commission of Health [grant numbers MS201736, Q201938], and Jiangsu Commission of Health [grant number H2019103].

ORCID iD

Jinsong Zhang https://orcid.org/0000-0003-4305-5733

References

1. Djebali S, Davis CA, Merkel A, et al. Landscape of transcription in human cells. *Nature* 2012; 489: 101–108.
2. Derrien T, Johnson R, Bussotti G, et al. The GENCODE v7 catalog of human long noncoding RNAs: analysis of their gene structure, evolution, and expression. *Genome Res* 2012; 22: 1775–1789.
3. Cloutier SC, Wang S, Ma WK, et al. Regulated formation of lncRNA-DNA hybrids enables faster transcriptional induction and environmental adaptation. *Mol Cell* 2016; 61: 393–404.
4. Li DY, Chen WJ, Luo L, et al. Prospective lncRNA-miRNA-mRNA regulatory network of long non-coding RNA LINC00968 in non-small cell lung cancer A549 cells: A miRNA microarray and bioinformatics investigation. *Int J Mol Med* 2017; 40: 1895–1906.
5. Liu H, Ren G, Hu H, et al. LPI-NRLMF: lncRNA-protein interaction prediction by neighborhood regularized logistic matrix factorization. *Oncotarget* 2017; 8: 103975–103984.
6. Zhang X, Zhang Y, Mao Y, et al. The lncRNA PCAT1 is correlated with poor prognosis and promotes cell proliferation, invasion, migration and EMT in osteosarcoma. *Onco Targets Ther* 2018; 11: 629–638.
7. Wang Y and Kong D. Knockdown of lncRNA MEG3 inhibits viability, migration, and invasion and promotes apoptosis by sponging miR-127 in osteosarcoma cell. *J Cell Biochem* 2018; 119: 669–679.
8. Qin Y, Sun W, Zhang H, et al. LncRNA GAS8-AS1 inhibits cell proliferation through ATG5-mediated autophagy in papillary thyroid cancer. *Endocrine* 2018; 59: 555–564.
9. Wu J, Cheng G, Zhang C, et al. Long noncoding RNA LINC01296 is associated with poor prognosis in prostate cancer and promotes cancer-cell proliferation and metastasis. *Onco Targets Ther* 2017; 10: 1843–1852.
10. Seitz AK, Christensen LL, Christensen E, et al. Profiling of long non-coding RNAs identifies LINC00958 and LINC01296 as candidate oncogenes in bladder cancer. *Sci Rep* 2017; 7: 395.
11. Yang Y, Junjie P, Sanjun C, et al. Long noncoding RNAs in colorectal cancer: progression and future directions. *J Cancer* 2017; 8: 3212–3225.
12. Wei AW and Li LF. Long non-coding RNA SOX21-AS1 sponges miR-145 to promote the tumorigenesis of colorectal cancer by targeting MYO6. *Biomed Pharmacother* 2017; 96: 953–959.
13. Qiu JJ and Yan JB. Long non-coding RNA LINC01296 is a potential prognostic biomarker in patients with colorectal cancer. *Tumour Biol* 2015; 36: 7175–7183.
14. Liu B, Pan S, Xiao Y, et al. LINC01296/miR-26a/GALNT3 axis contributes to colorectal cancer progression by regulating O-

glycosylated MUC1 via PI3K/AKT pathway. *J Exp Clin Cancer Res* 2018; 37: 316.
15. Georgakilas AG, Martin OA and Bonner WM. p21: a two-faced genome guardian. *Trends Mol Med* 2017; 23: 310–319.
16. Xu XL, Wu LC, Du F, et al. Inactivation of human SRBC, located within the 11p15.5-p15.4 tumor suppressor region, in breast and lung cancers. *Cancer Res* 2001; 61: 7943–7949.
17. Heidenreich B, Heidenreich A, Sesterhenn A, et al. Aneuploidy of chromosome 9 and the tumor suppressor genes p16(INK4) and p15(INK4B) detected by in situ hybridization in locally advanced prostate cancer. *Eur Urol* 2000; 38: 475–482.
18. Markus J, Garin MT, Bies J, et al. Methylation-independent silencing of the tumor suppressor INK4b (p15) by CBFbeta-SMMHC in acute myelogenous leukemia with inv (16). *Cancer Res* 2007; 67: 992–1000.
19. Hutter G, Scheubner M, Zimmermann Y, et al. Differential effect of epigenetic alterations and genomic deletions of CDK inhibitors [p16(INK4a), p15(INK4b), p14(ARF)] in mantle cell lymphoma. *Genes Chromosomes Cancer* 2004; 45: 203–210.
20. Kudoh K, Ichikawa Y, Yoshida S, et al. Inactivation of p16/CDKN2 and p15/MTS2 is associated with prognosis and response to chemotherapy in ovarian cancer. *Int J Cancer* 2001; 99: 579–582.
21. Ishiguro A, Takahata T, Saito M, et al. Influence of methylated p15 and p16 genes on clinicopathological features in colorectal cancer. *J Gastroenterol Hepatol* 2006; 21: 1334–1339.
22. Nienstedt JC, Schroeder C, Clauditz T, et al. EZH2 overexpression in head and neck cancer is related to lymph node metastasis. *J Oral Pathol Med* 2018; 47: 240–245.
23. Chen Z, Yang P, Li W, et al. Expression of EZH2 is associated with poor outcome in colorectal cancer. *Oncol Lett* 2018; 15: 2953–2961.
24. Lian Y, Yan C, Ding J, et al. A novel lncRNA, LL22NC03-N64E9.1, represses KLF2 transcription through binding with EZH2 in colorectal cancer. *Oncotarget* 2017; 8: 59435–59445.
25. Ba MC, Long H, Cui SZ, et al. Long noncoding RNA LINC00673 epigenetically suppresses KLF4 by interacting with EZH2 and DNMT1 in gastric cancer. *Oncotarget* 2017; 8: 95542–95553.